

A COMPREHENSIVE STUDY OF THE PHOTOSPHERIC MAGNETIC FIELD CHANGE ASSOCIATED WITH SOLAR FLARES

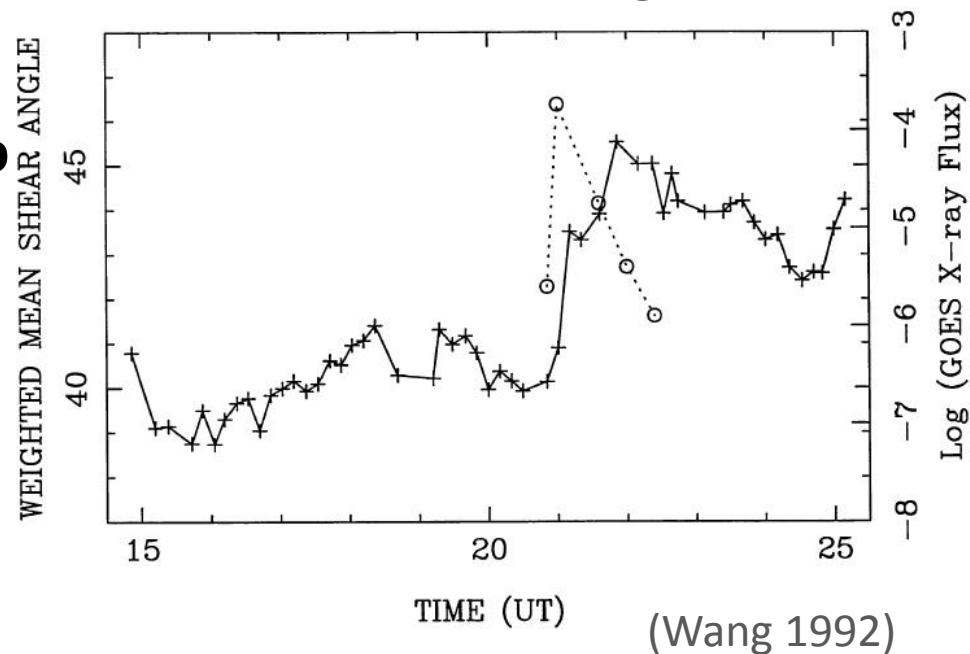
Shuo Wang¹, Chang Liu¹, Na Deng¹, Rui Liu¹, Yang Liu², Haimin Wang¹
1. New Jersey Institute of Technology, Newark, NJ, United States.
2. Stanford University, Stanford, CA, United States.

Discovery

2

☞ **Rapid and permanent enhancement of transverse magnetic fields near the flaring magnetic polarity inversion line associated with flares were discovered two decades ago** (Wang 1992; Wang et al. 1994).

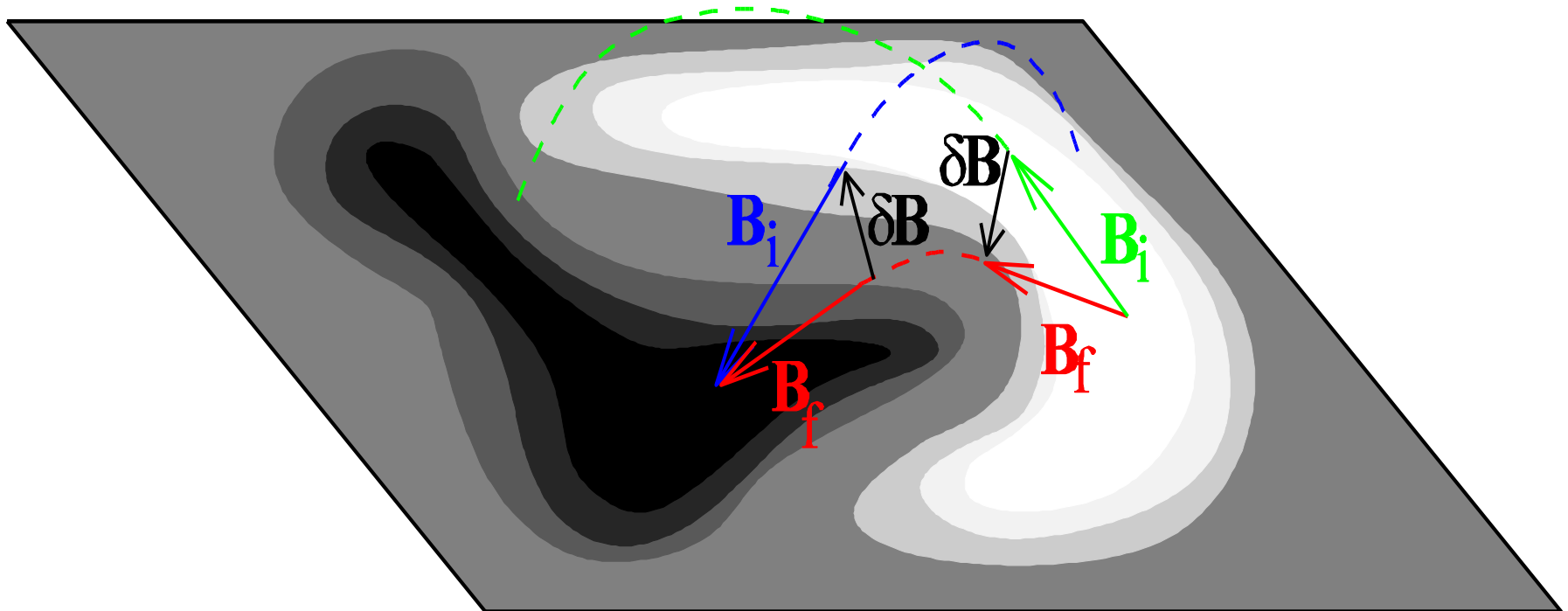
☞ **Similar trend has continued to be observed later on in many observations** (Wang et al., 2002, 2004, 2005; Liu et al., 2005; Wang et al., 2007; Jing et al., 2008; Li et al., 2009; Liu et al., 2011), **and shows some agreement with recent MHD modeling** (Li et al., 2011).



Implosion Model

3


- ∞ The coronal magnetic field should contract inward, as the magnetic energy decreases after flares/CMEs (Hudson, 2000).
- ∞ Conservation of momentum.

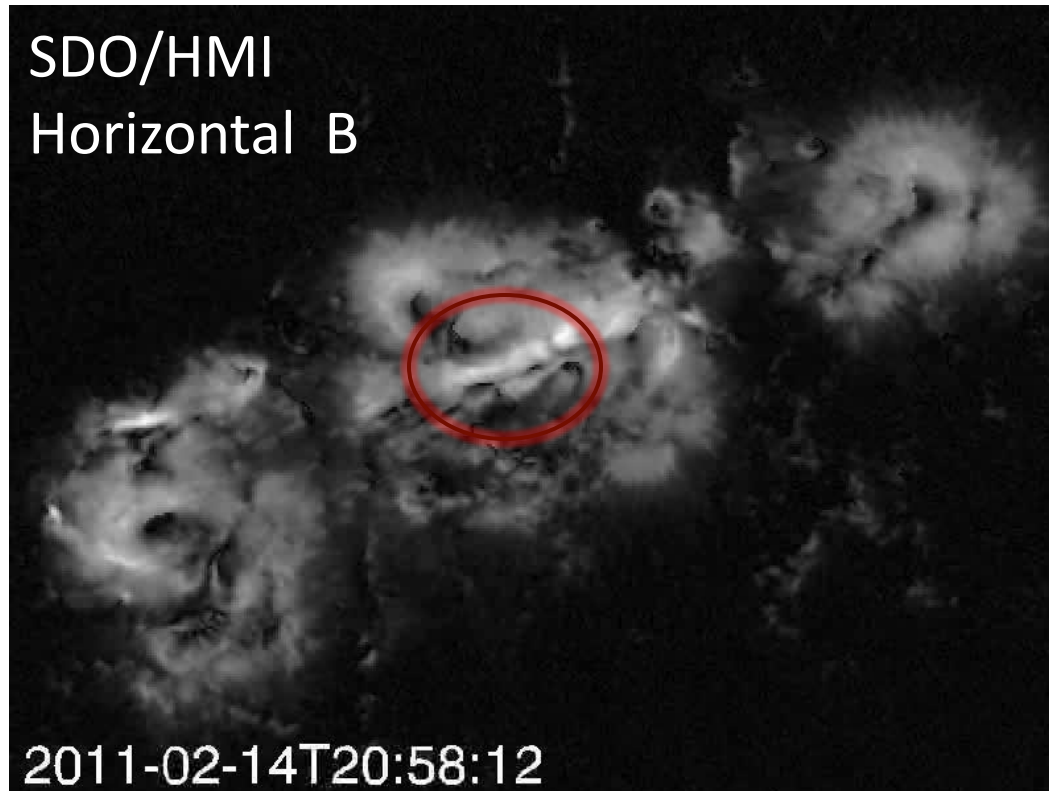


(Hudson et al. 2008)

Magnetic Field Change Observed by SDO/HMI

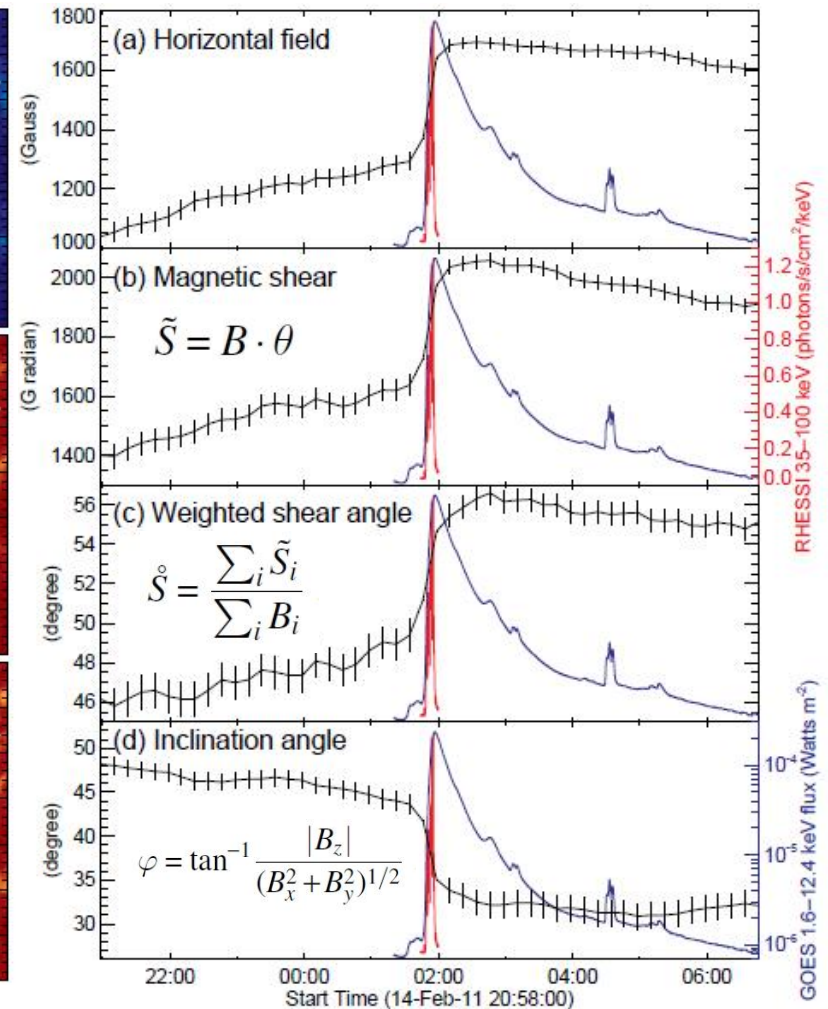
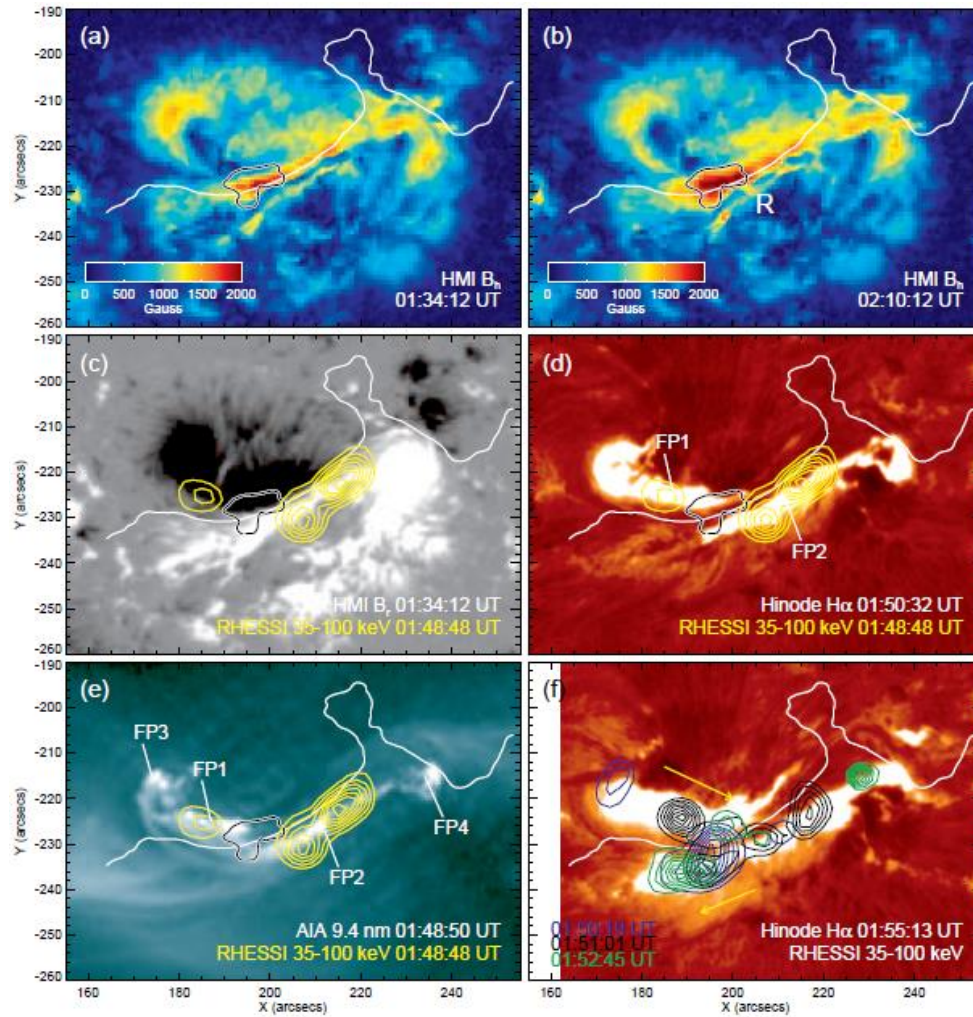
4

 2011 Feb 15 X2.2 flare



Magnetic Field Change Observed by SDO/HMI

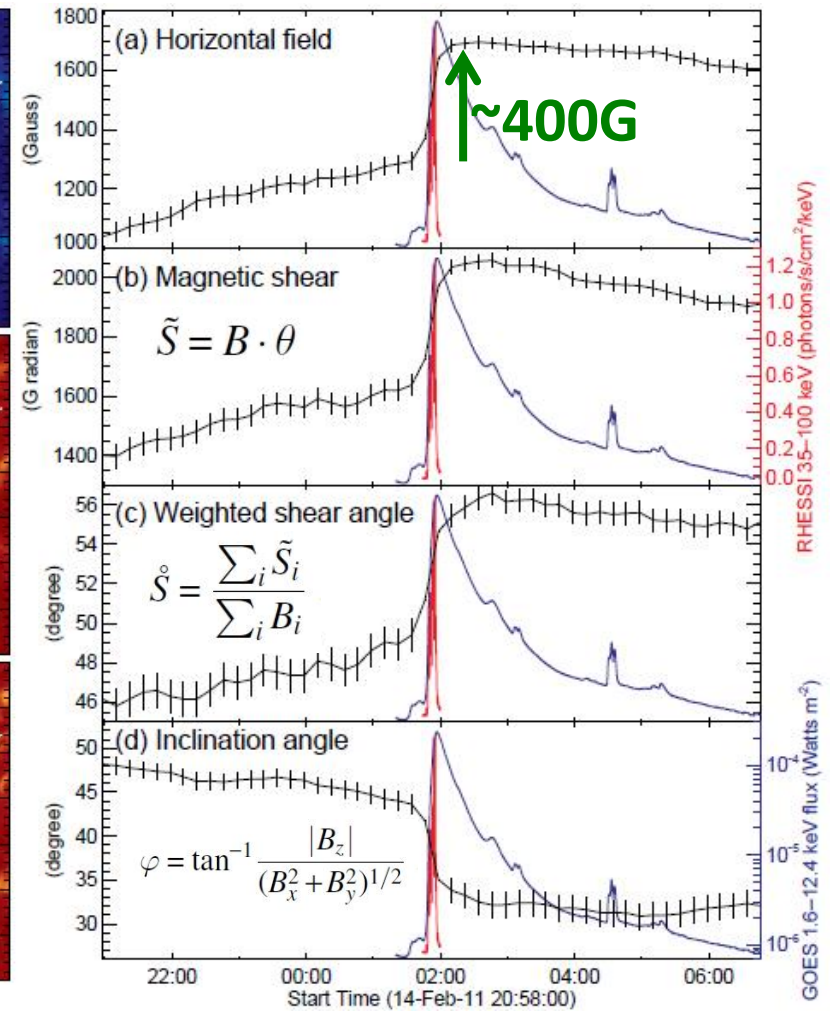
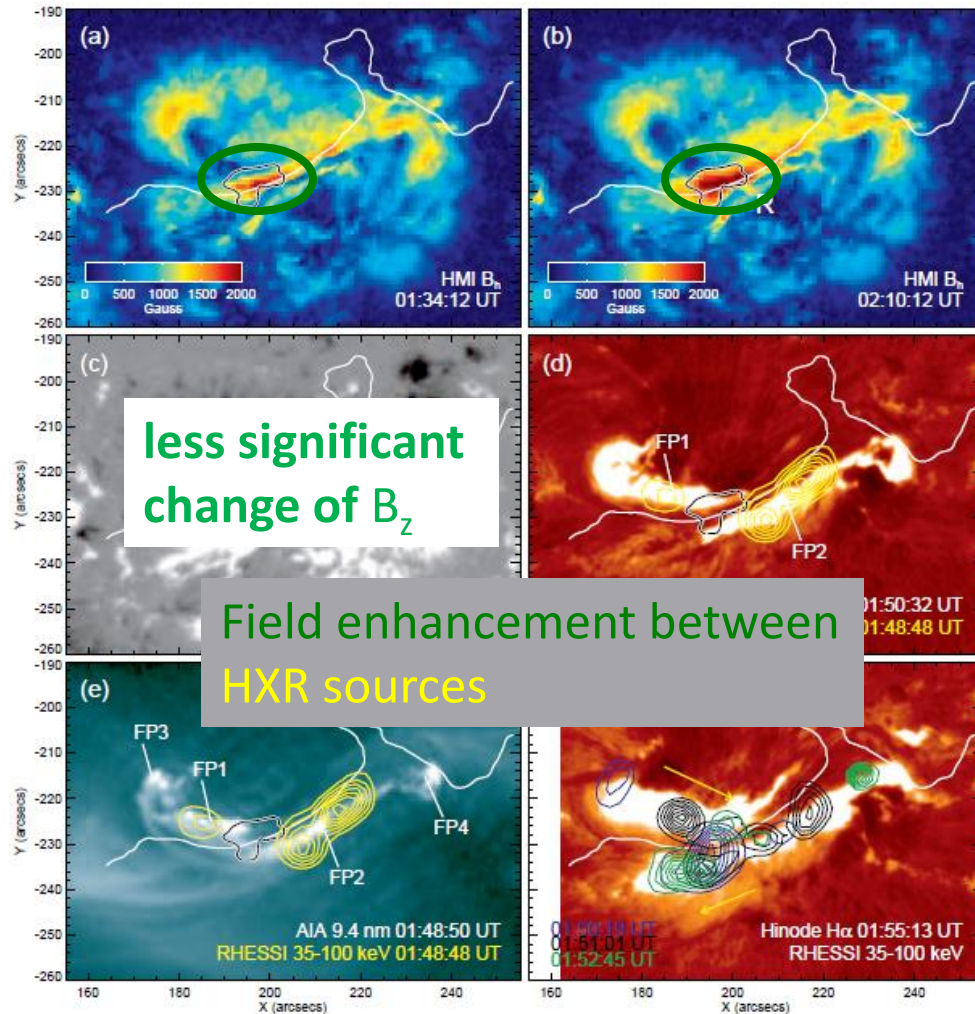
5



Wang et al., 2012, ApJ, 745, L17.

Magnetic Field Change Observed by SDO/HMI

6



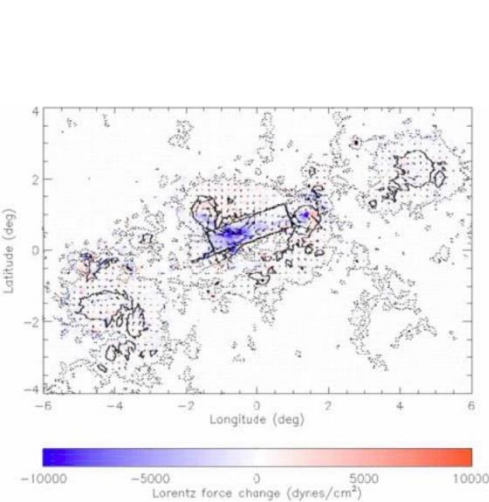
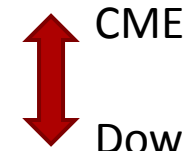
Change of Lorentz Force

7

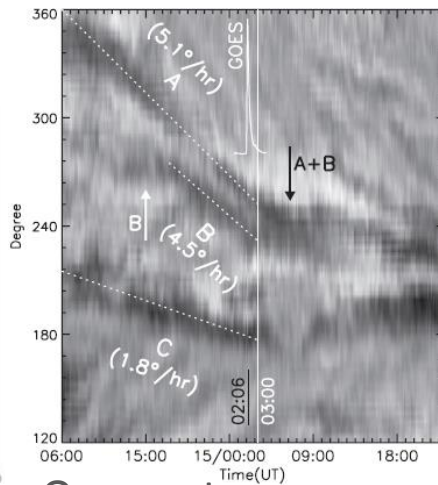
$$\delta F_{r,\text{interior}} = \frac{1}{8\pi} \int_{A_{\text{ph}}} dA (\delta B_r^2 - \delta B_h^2)$$

$$\delta \mathbf{F}_{h,\text{interior}} = \frac{1}{4\pi} \int_{A_{\text{ph}}} dA \delta (B_r \mathbf{B}_h)$$

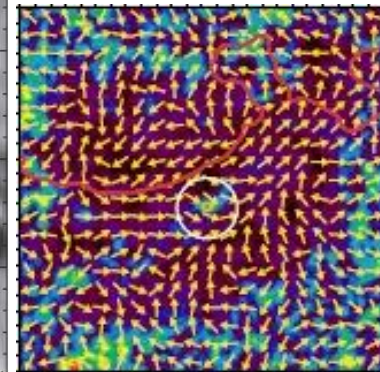
(Fisher et al., 2012)



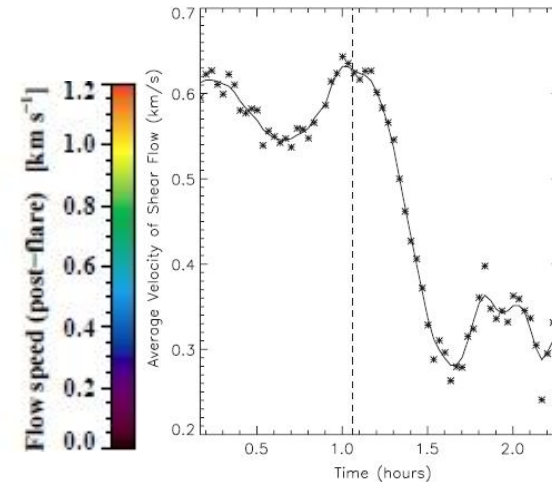
Lorentz force direction (Petrie, 2012)



One spot rotational speed (Jiang et al., 2012)



Shear flow difference before and after flare (Beauregard et al., 2011)

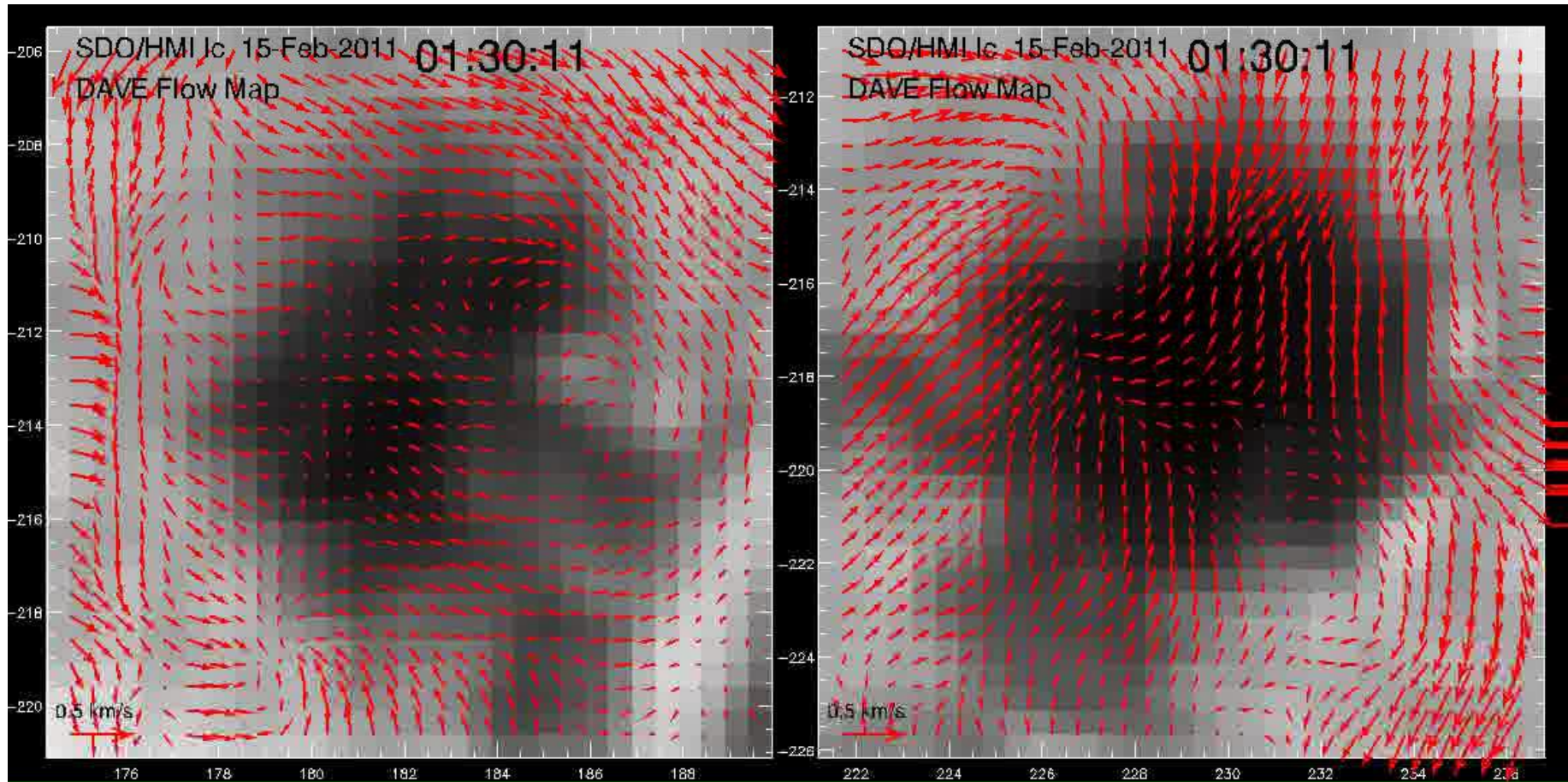


Shear flow decrease after flare in AR 10930 (Tan et al., 2009)

Sudden Acceleration of Spots Rotation

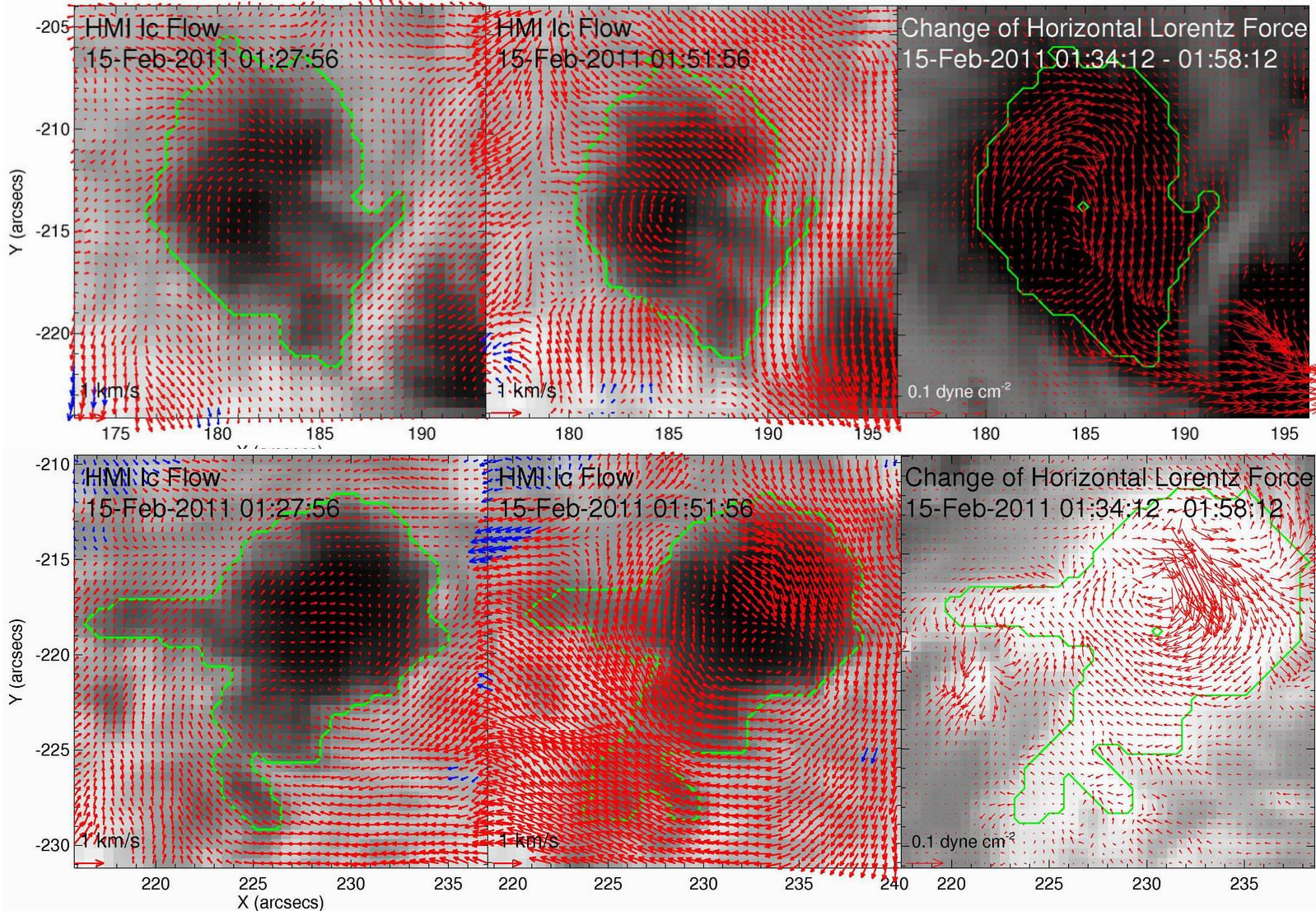
8

DAVE method (Schuck 2006) applied to obtain surface flow.



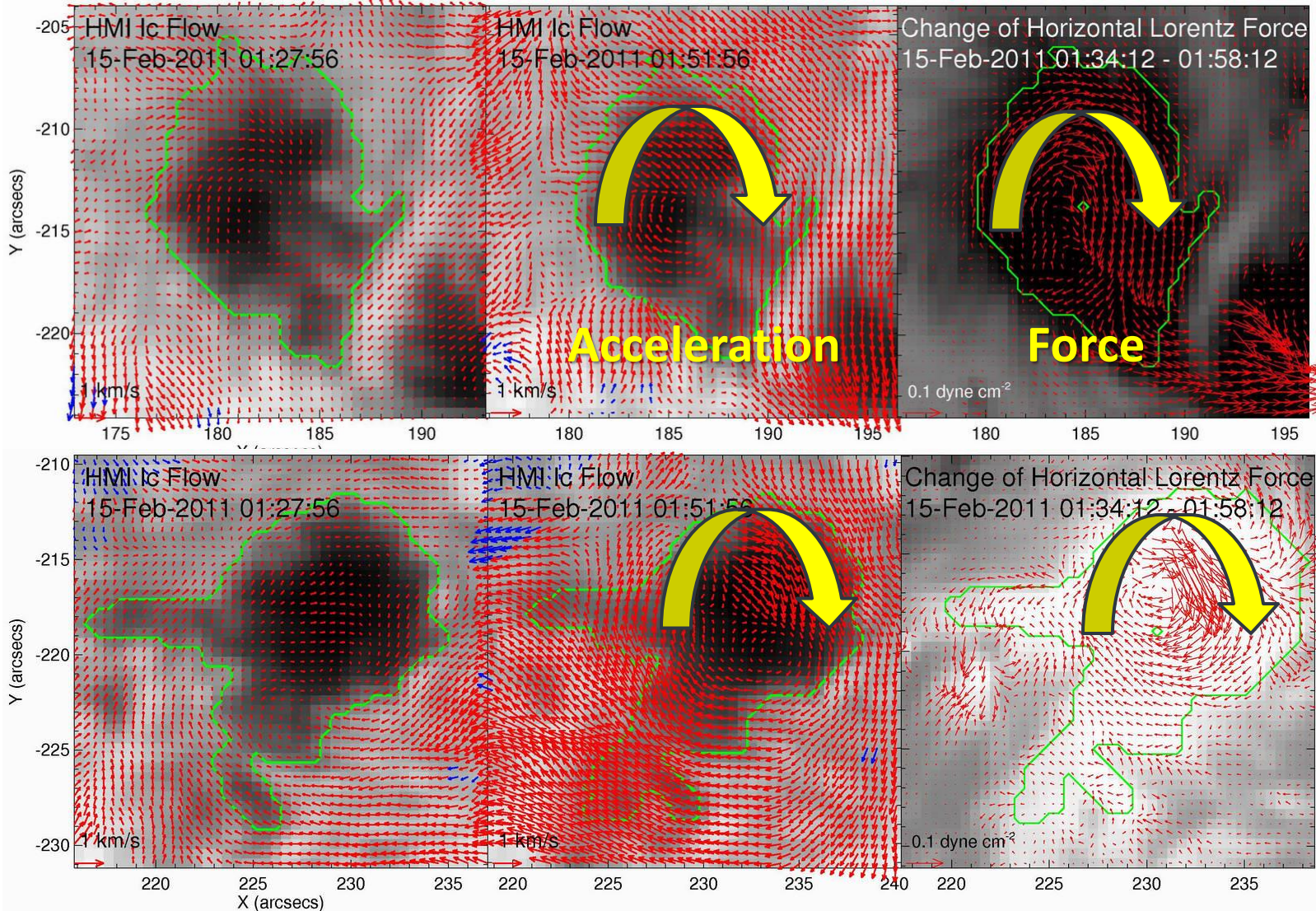
Lorentz Force as Driving Force

9



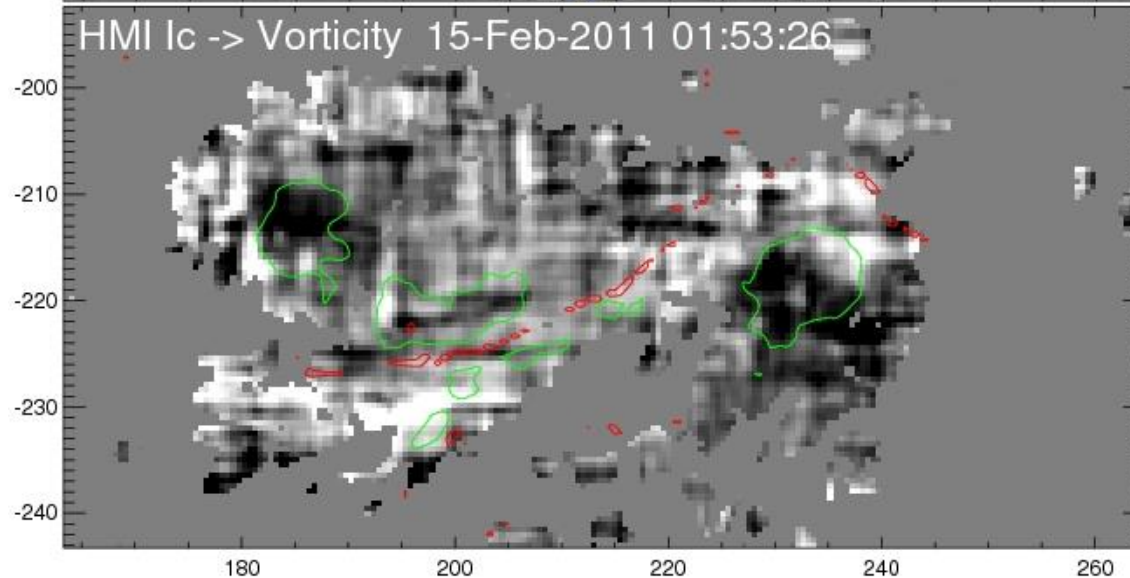
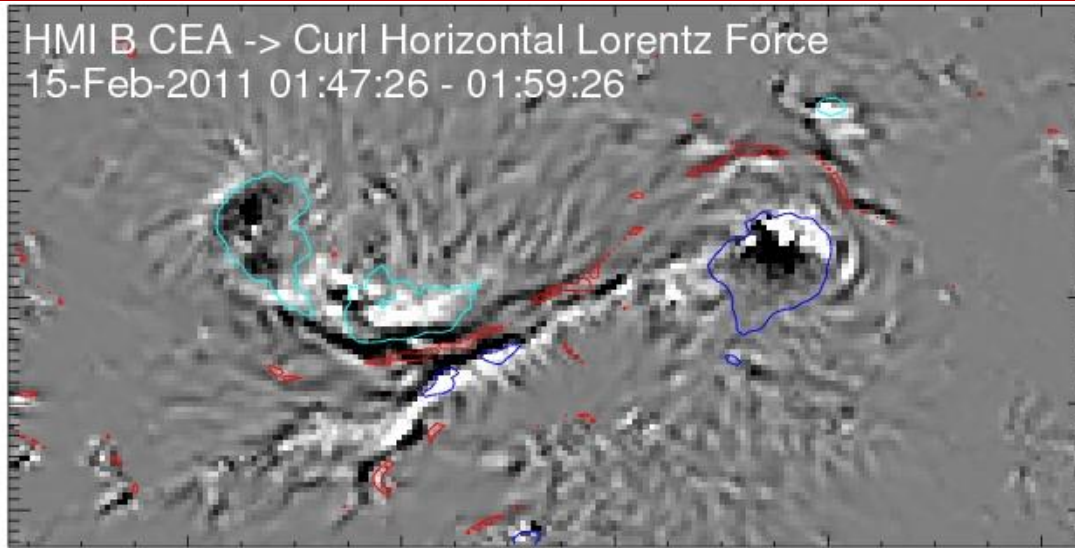
Lorentz Force as Driving Force

10

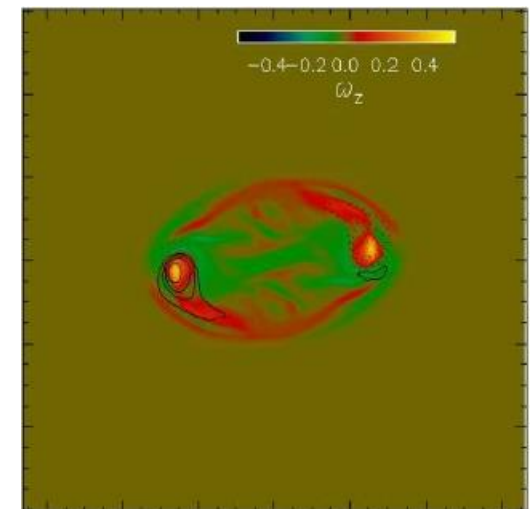


Vorticity & Curl Lorentz Force

11

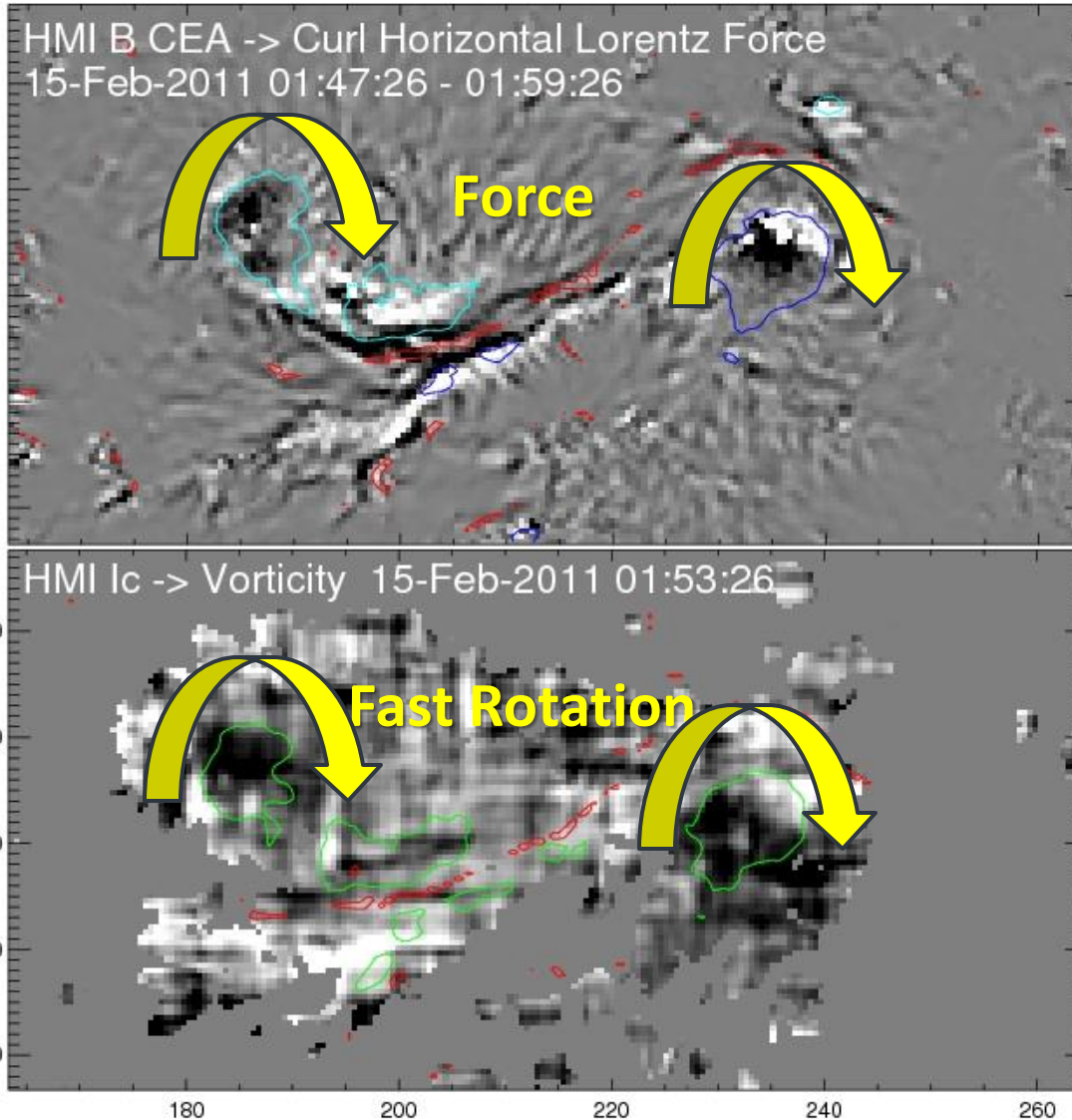


The vorticity map is consistent with the twisted flux tube eruption simulation (Fan 2009).

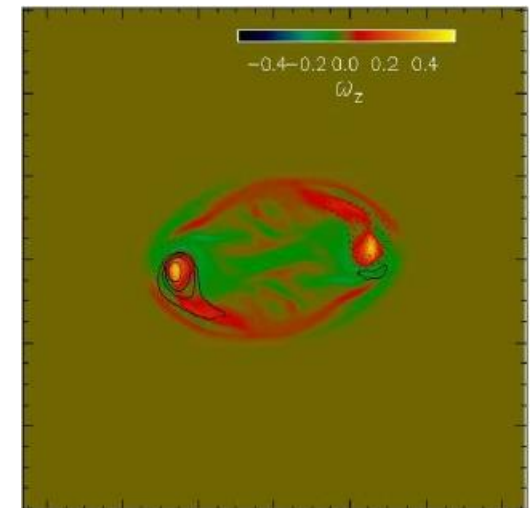


Vorticity & Curl Lorentz Force

12

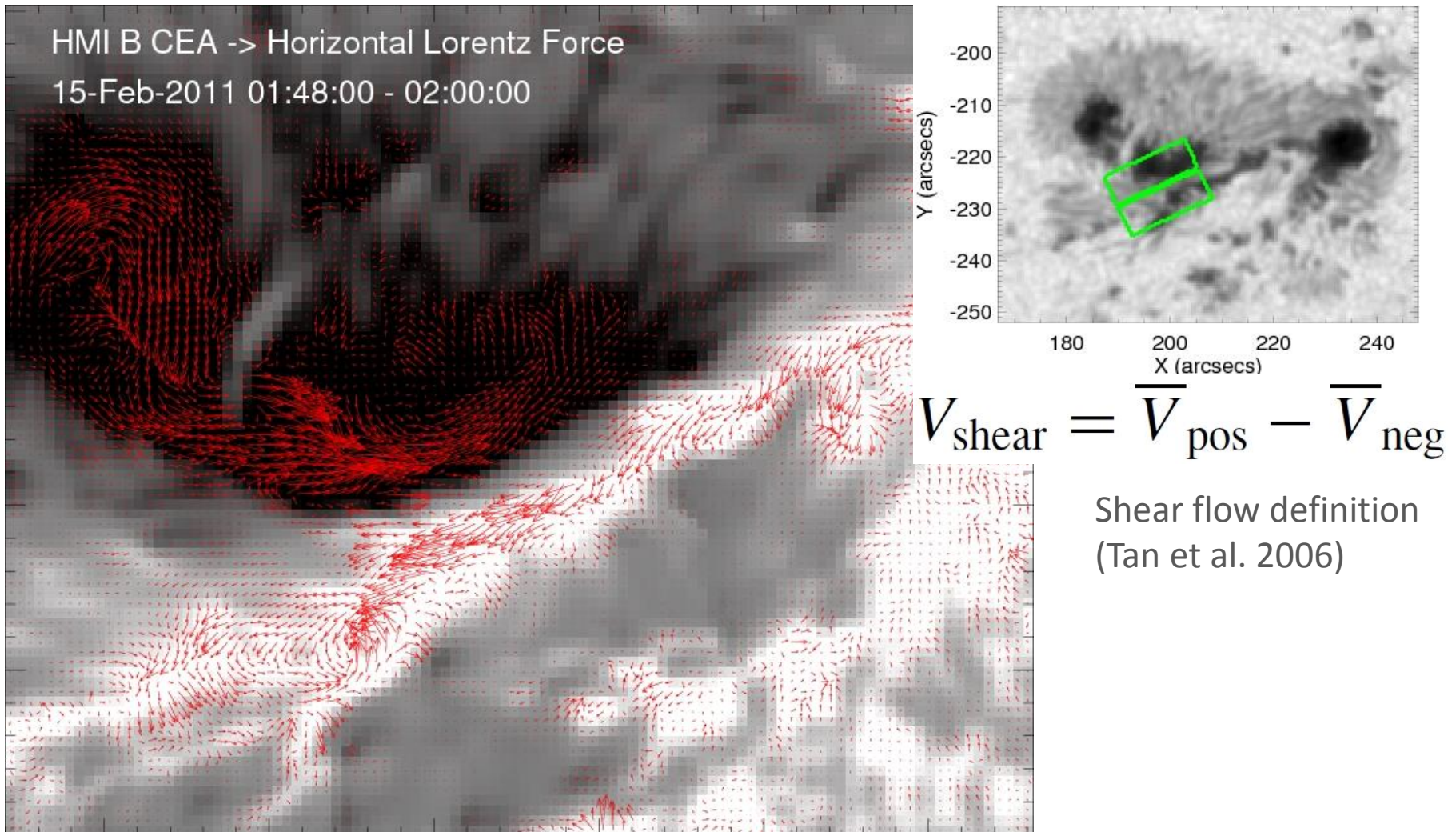


The vorticity map is consistent with the twisted flux tube eruption simulation (Fan 2009).



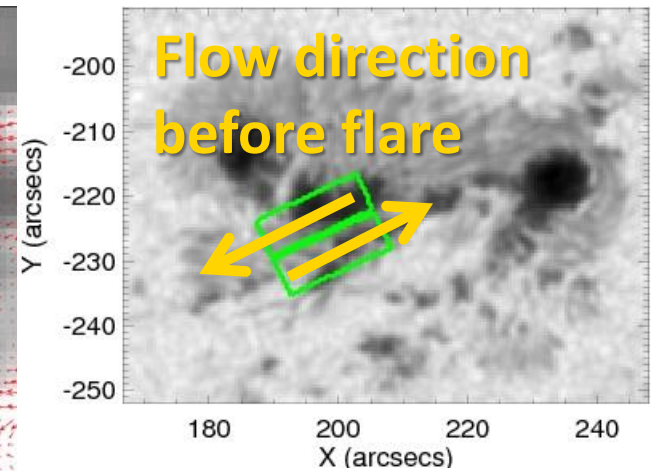
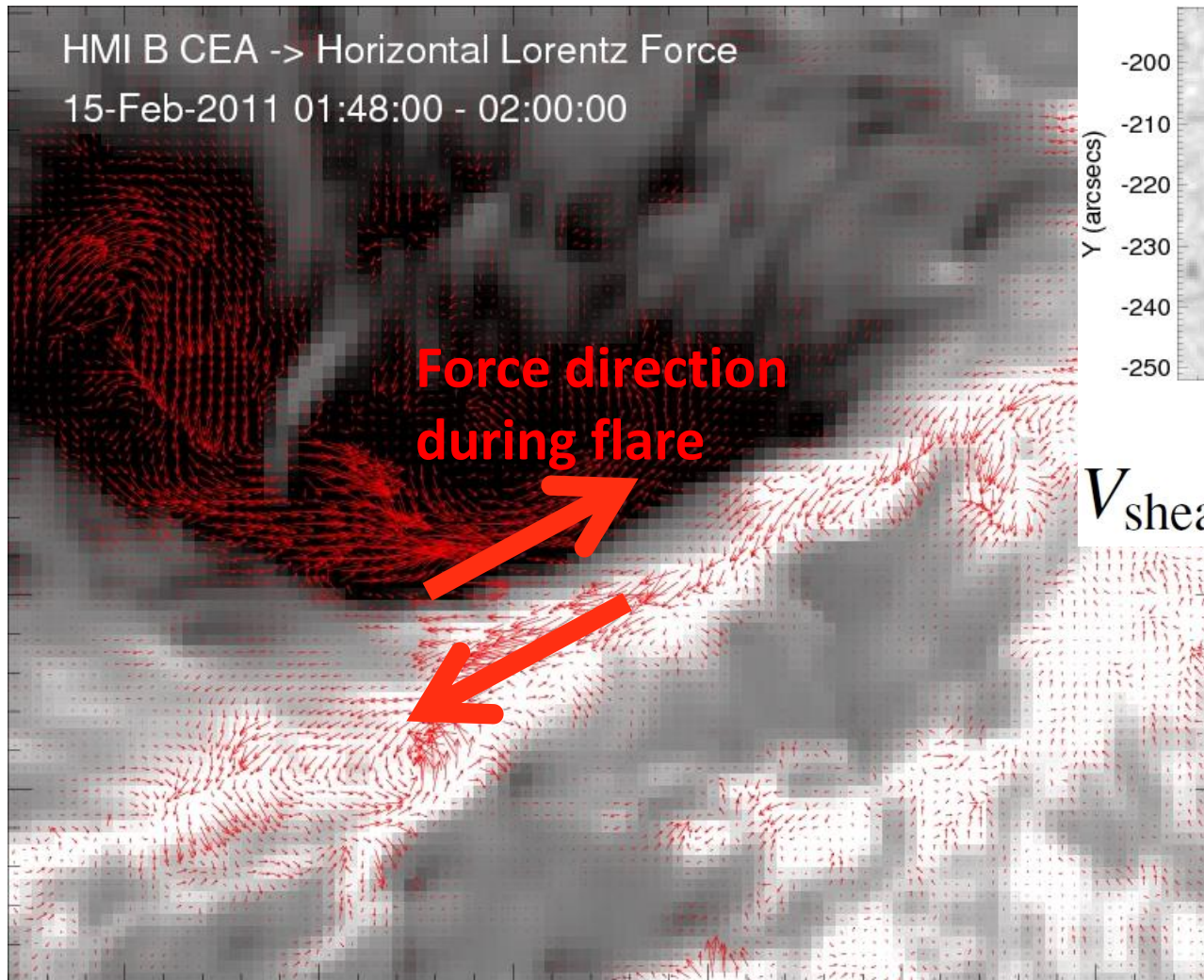
Shear Flow Decrease

13



Shear Flow Decrease

14

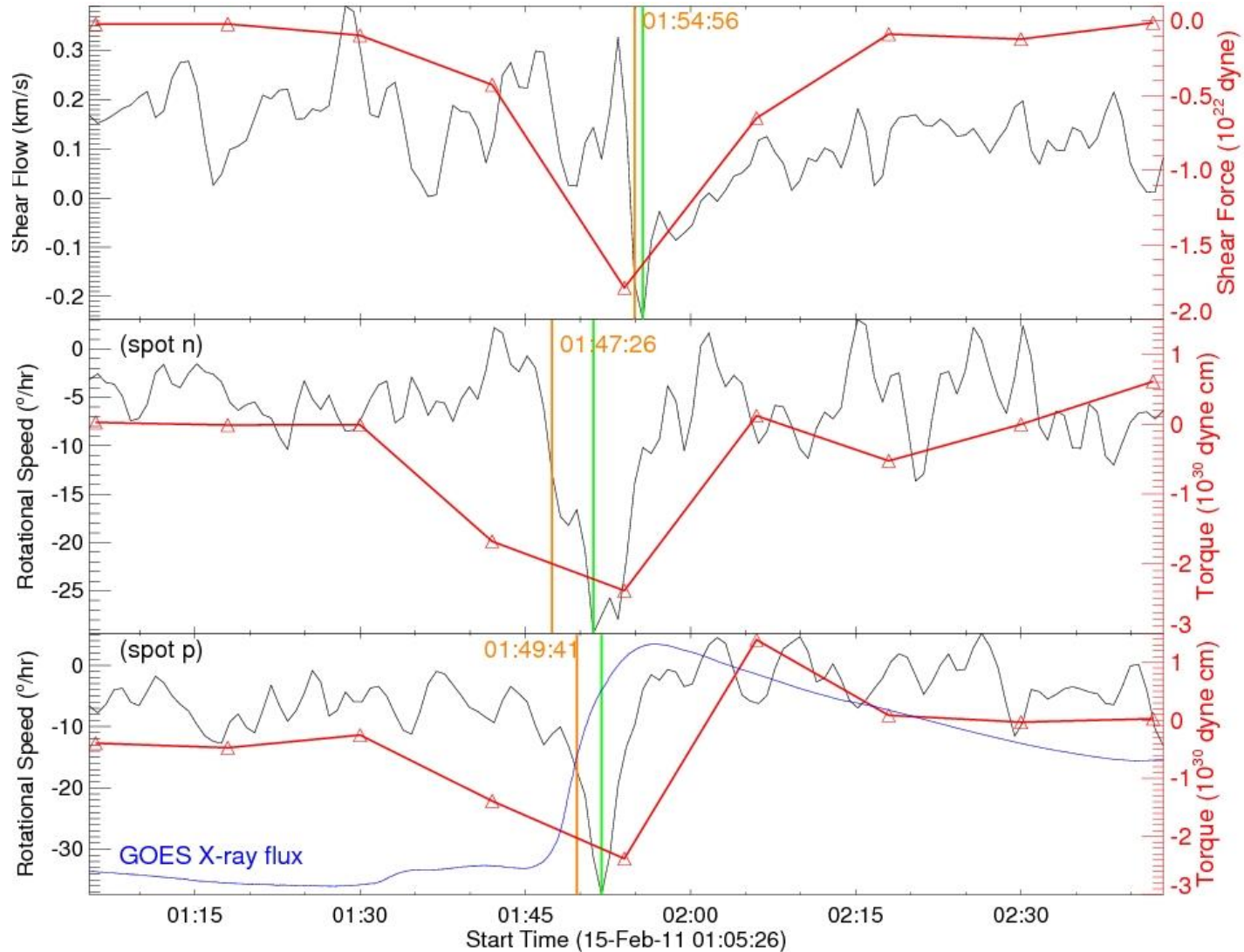


$$V_{\text{shear}} = \overline{V}_{\text{pos}} - \overline{V}_{\text{neg}}$$

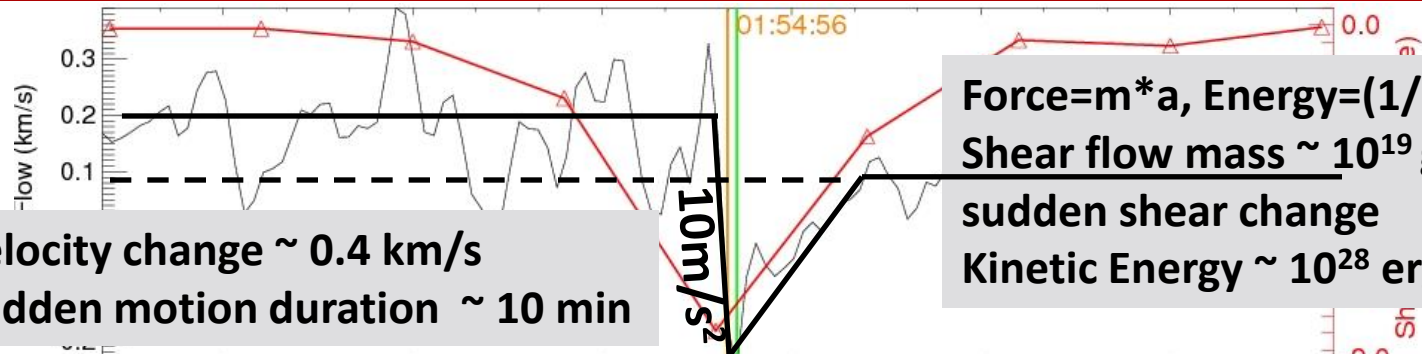
Shear flow definition
(Tan et al. 2006)

Sudden Motion & Force

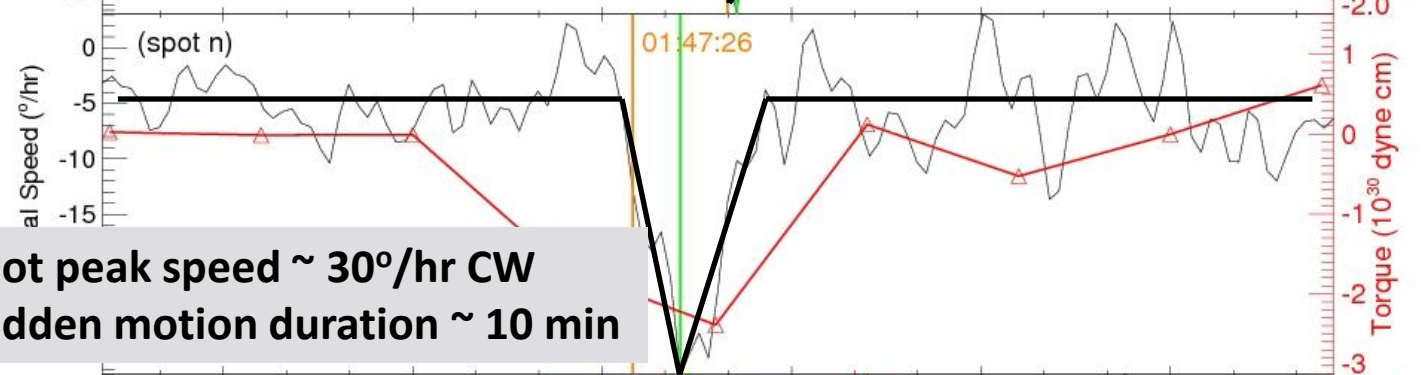
15



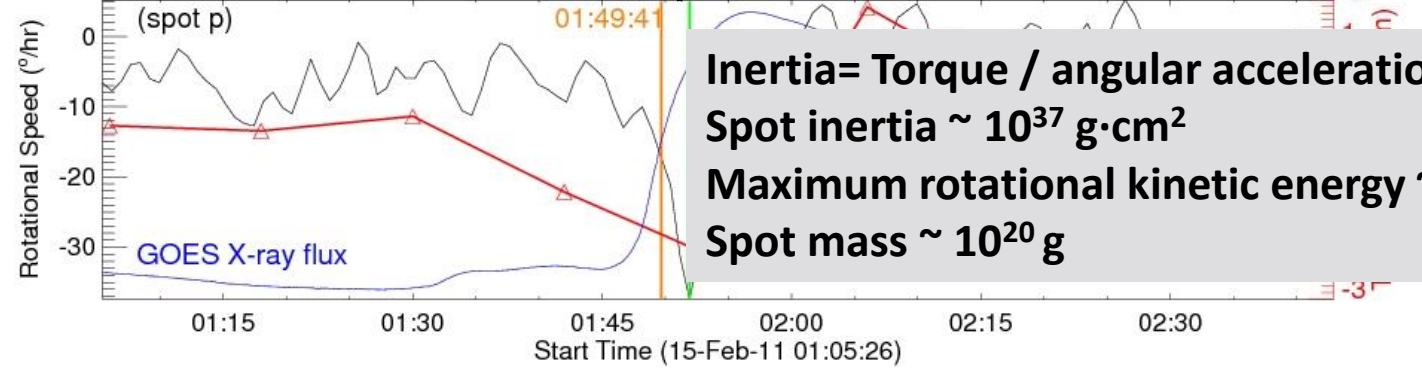
Sudden Motion & Force



Force = $m \cdot a$, Energy = $(1/2) \cdot m \cdot v^2$
Shear flow mass $\sim 10^{19}$ g
sudden shear change
Kinetic Energy $\sim 10^{28}$ erg




Spot peak speed $\sim 30^\circ/\text{hr}$ CW
Sudden motion duration ~ 10 min




Inertia = Torque / angular acceleration
Spot inertia $\sim 10^{37}$ g·cm²
Maximum rotational kinetic energy $\sim 10^{29}$ erg
Spot mass $\sim 10^{20}$ g

More Cases

17


 The horizontal field enhancement at the flaring PIL and rotational field change of nearby spots are common.


 The shear and rotational motions are consistent with the field changes.

Date [yymmdd]	Flare Class
110213	M6.6
110215	X2.2
110906	M5.3
110906	X2.1
110907	X1.8
110925	M7.4
120307	X1.3
120307	X5.4
120309	X1.5
120510	M5.7
120712	X1.4

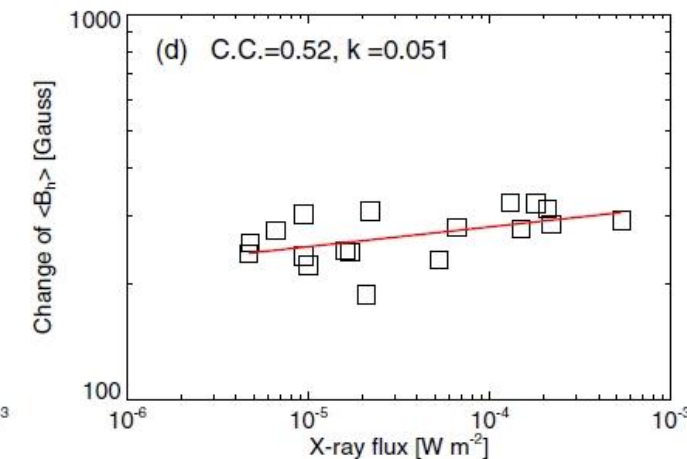
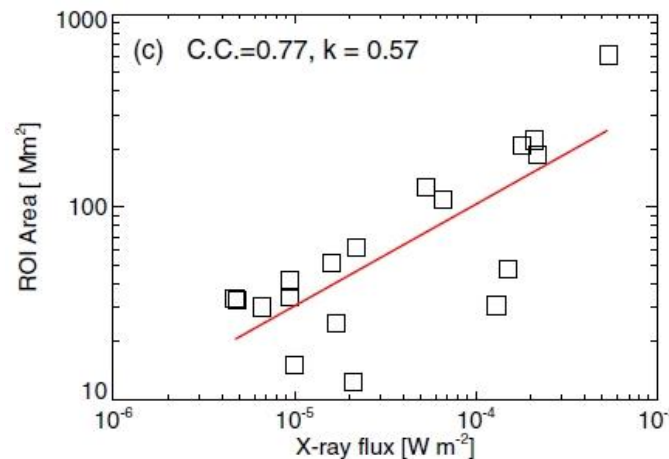
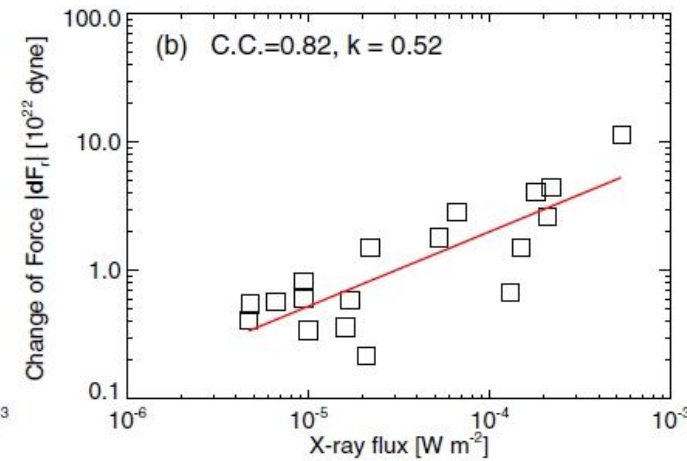
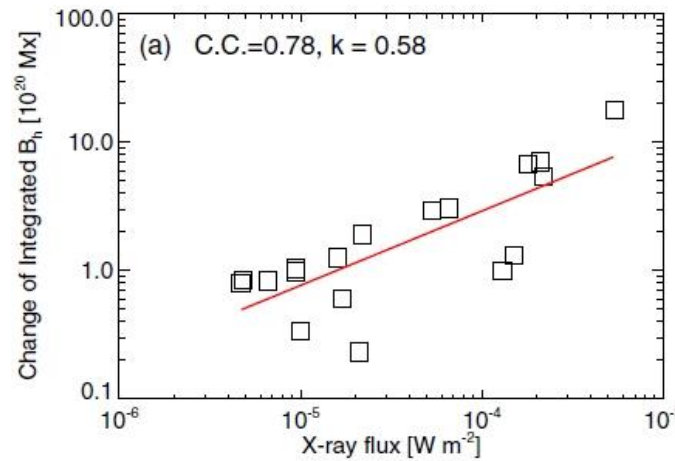
Statistical Results

18

18 flares with horizontal field enhancement

co-temporal with the flare initiation

co-spatial with the PIL between the two main flare kernels

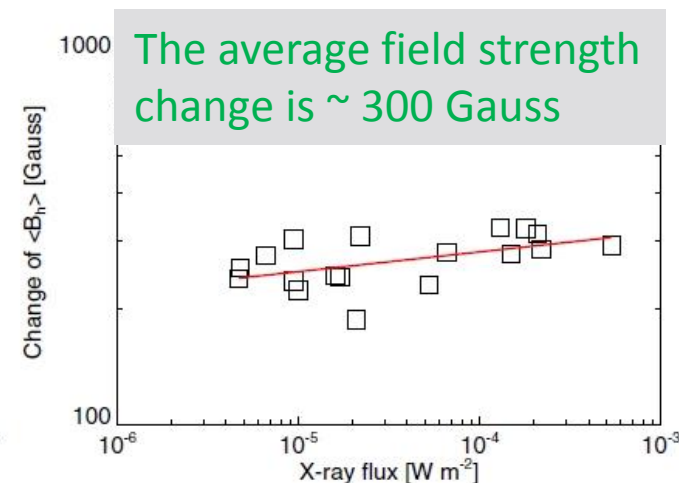
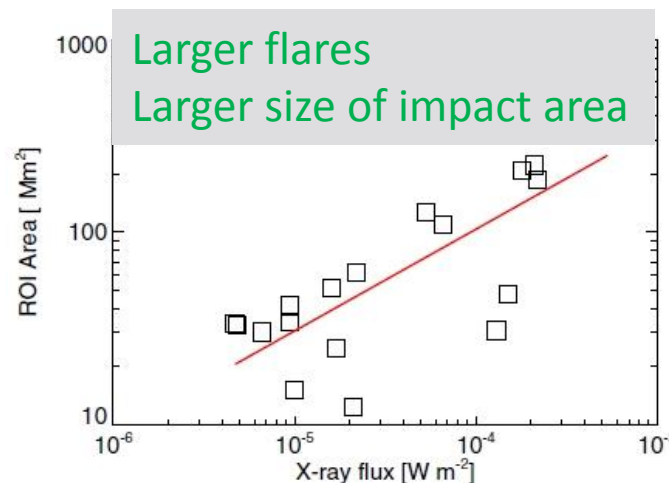
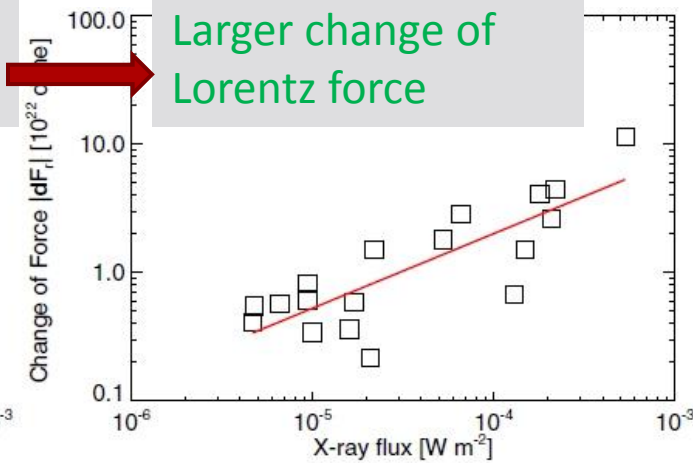
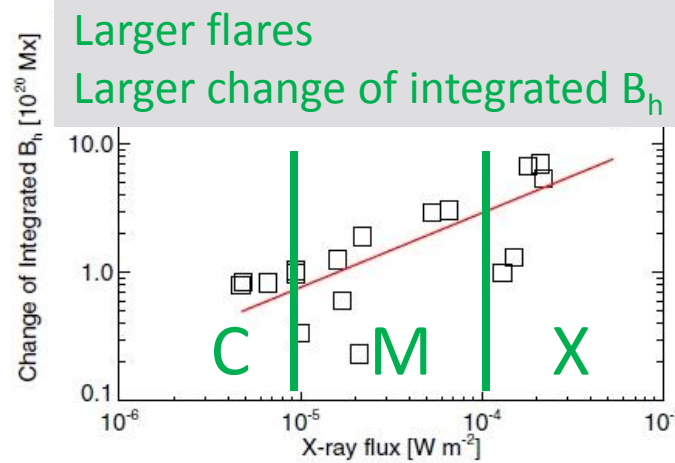


Wang et al., 2012, ApJ, 757, L5.

Statistical Results

19

18 flares with horizontal field enhancement
co-temporal with the flare initiation
co-spatial with the PIL between the two main flare kernels



Wang et al., 2012, ApJ, 757, L5.

CME Mass Estimation

20


Momentum conservation

$$M_{\text{CME}} \simeq \frac{1}{2} \frac{\delta F_r \delta t}{v}$$
 (Fisher et al., 2012)

<i>GOES</i> 1–8 Å Peak (UT)	NOAA AR	<i>GOES</i> Class	CME Time (UT)	CME Speed (km s ⁻¹)	CME Mass (10 ¹⁵ g)
2011 Feb 13 17:38	11158	M6.6	18:36	373	3.8
2011 Feb 14 17:26	11158	M2.2	18:24	326	2.3
2011 Feb 15 01:56	11158	X2.2	02:24	669	3.3
2011 Sep 06 01:50	11283	M5.3	02:24	782	1.2
2011 Sep 06 22:20	11283	X2.1	23:05	575	2.3
2011 Sep 07 22:38	11283	X1.8	23:05	792	2.6

Notes. Information of the CME time (the first C2 appearance time) and the CME speed are from LASCO CME catalog. The masses were computed assuming $\delta t = 10$ s

Wang et al., 2012, ApJ, 757, L5.

Summary

21

Rapid and permanent horizontal magnetic field change in the photosphere during flares

- Enhancement around flaring magnetic polarity inversion line confirmed with SDO/HMI data
- Accompanied with magnetic field rotational changes in major flares
- Observed down to C4 class flares
- Correlations between the peak GOES X-ray flux and the size of the affected area / integrated field change / Lorentz force change

Sudden motions in the photosphere during flares

- Shear flows along PILs sharply decrease
- Sudden rotation of spots

Lorentz force change implied by magnetic field change is the driving force of these sudden motions.

- CME mass estimation
- Estimation of shear flow mass/energy, spot mass/inertia/rotational energy